MICRO-INFRARED AND MICRO-RAMAN SPECTROSCOPIES OF SUTTER'S MILL METEORITE GRAINS. M. Yesiltas[1], Y. Kebukawa[2], E. Mattson[3], C. J. Hirschmugl[3], R. E. Peale[1], [1]Dept. of Physics, University of Central Florida, PS 430, Orlando, FL, 32816, (myesiltas@knights.ucf.edu), [2]Dept. of Natural History Sciences, Hokkaido University, Sapporo, Japan 060-0810, [3]Dept. of Physics, University of Wisconsin-Milwaukee, Milwaukee, WI, 53211.

Introduction: Sutter's Mill (SM) meteorite fell in El Dorado County, California on 22 April 2012. First samples were recovered on 24 April 2012 [1]. A few days after the fall, it rained heavily, after which more fragments were recovered. SM is classified as a CM chondrite. Among fragments, SM presents multiple lithologies as well as signatures of aqueous alteration and thermal metamorphism of varying degree [1]. We present *in-situ* investigation of SM2 and SM12 meteorite fragments by (i) synchrotron-based Fourier transform infrared (FTIR) microspectroscopy, and (ii) micro-Raman spectroscopy.

Samples: We received fragments of SM2 and SM12 in the form of chips from the Sutter's Mill meteorite consortium. SM2 was recovered prior to the rains in the fragmented form by P. Jenniskens on 24 April 2012. SM12 was exposed to the rain, and recovered by M. Waiblinger on 29 April 2012. We further ground both samples in a mortar and pestle down to micrometer size grains. Subsequently, these grains were dropped onto a diamond window which is placed under the microscope for transmission measurements, and onto a silicon substrate for micro-Raman measurements.

Methods: The FTIR microspectroscopy experiments were performed at the Synchrotron Radiation Center in Stoughton WI, using the IRENI beamline [2]. The setup is comprised of a Bruker Hyperion 3000 IR microscope and a Bruker Vertex 70 FTIR spectrometer. Transmission measurements were performed using a 74× magnification objective. The effective 0.54 × 0.54 μm^2 pixel size provides spatially resolved images that are diffraction-limited at all wavelengths. Spectra were recorded with 4 cm^{-1} resolution using 128 co-added scans. A clean and sample-free region of the diamond window was used for reference spectra. Micro-Raman spectra of Sutter's Mill samples were collected at the Materials Characterization Facility at the University of Central Florida using a Renishaw spectrometer coupled to Leica DMLM microscope with Ar-ion laser excitation at 514.5 nm wavelength. A 5× objective was used to locate a meteorite grain of interest. Then a 50× objective was used to collect the spectrum.

Results: Fig. 1 presents grain-averaged mid-infrared spectra for individual grains of SM2 and SM12, indicating highly heterogeneous composition. SM2 spectra contain an unresolved triplet near 1000 cm^{-1} with grain-to-grain variations in the contributions from olivine, pyroxene, and phyllosilicates. In contrast, the same spectral region for SM12 grains shows only a single broad band due to phyllosilicates. Most spectra also exhibit a broad band around 1500-1400 cm^{-1} due to asymmetric stretching of carbonate CO_3, a 1640 cm^{-1} band due to H-O-H bending, and a broad band around 3700-3000 cm^{-1} due to O-H stretching.

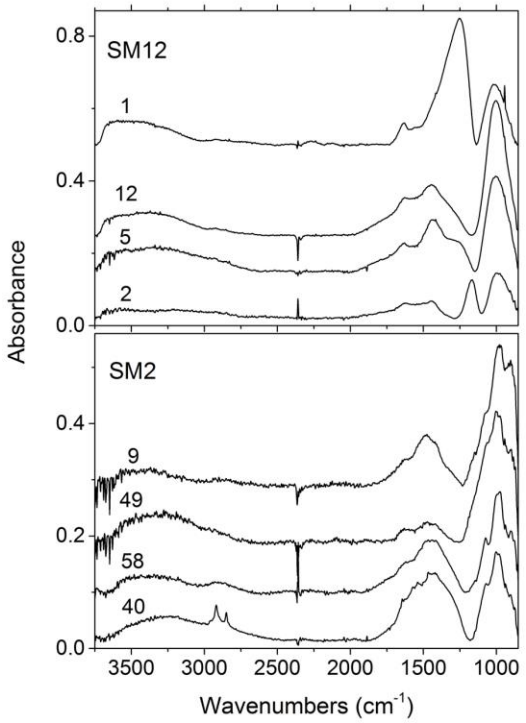

Figure 1. Mid-infrared spectra of individual SM2 and SM12 grains. Labels enumerate grains in the field of view.

Spectra for some SM2 grains contain weak but sharp lines in the range of 3000-2800 cm^{-1} due to C-H stretching of aliphatic hydrocarbons. Band profiles for these features differ from those reported for SM2 in [4]. Aliphatic hydrocarbon features are less pronounced in our SM12 grains. Carbonate bands in spectra of SM2 grains appear to have more structure than those of SM12 in the 1400-1480 cm^{-1} region. Fig. 2 presents a plot of line widths for the Raman G-band (due to graphite-like sp2 carbon bonds) vs center frequency. The difference between SM2 and SM12 sug-

gests the latter is thermally more metamorphosed. We calculated effective peak metamorphism temperatures for SM2 and SM12 grains following [3] and obtained 130 - 260 C for SM2 and 280 - 310 C for SM12, which are 10 – 30% higher than the values reported in [1].

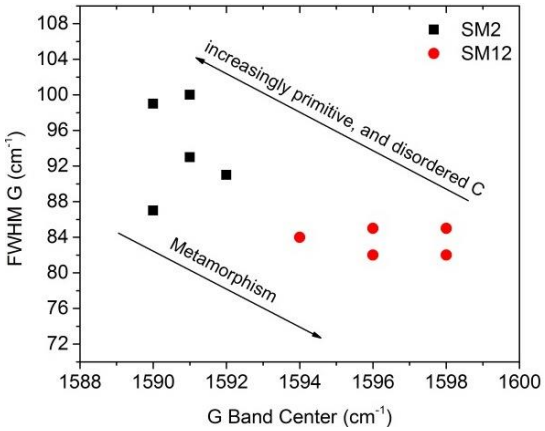

Figure 2. FWHM of G-band versus G-band center frequency for SM2 and SM12 grains.

Figure 3 presents a visible and an infrared image at 2850 cm^{-1} for a single SM2 grain. By integrating over specific wavenumber ranges, we obtain spatial maps of feature intensities within individual grains (as in [5, 6]), which reveal different distributions for organics and minerals. We find in an SM2 grain that aliphatic hydrocarbons spatially coincide with silicates but not with OH. Oppositely, we find for an SM12 grain that aliphatic hydrocarbons spatially coincide with OH but not with silicates.

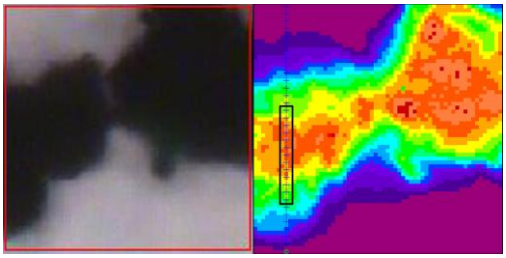

Figure 3. Visible micrograph (left), and infrared image (right) of an SM2 grain at 2850 cm^{-1}.

Figure 4 presents mid-infrared spectra extracted from the pixels along the vertical slice indicated in Fig. 3 (right). The mineral and organic compositions vary dramatically across this single grain. The silicate band (~ 1000 cm^{-1}) splits in two. The hydrocarbon lines appear correlated with the carbonate band. A band that appears in the second lowest curve near 3600 cm^{-1} can be attributed to fine grain phyllosilicates.

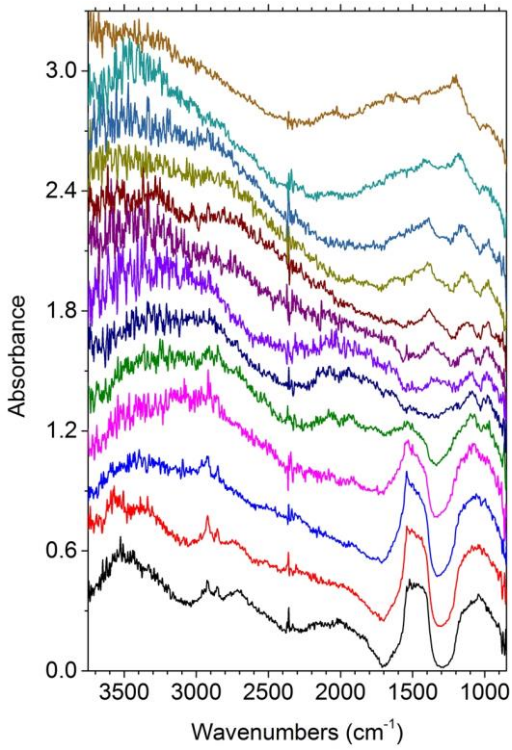

Figure 4. Spectra (bottom to top) of pixels along the vertical line (bottom to top) shown in the infrared image in Fig. 3. Individual spectrum is offset for clarity.

Conclusions: Infrared spectroscopy reveals strong differences in olivine, pyroxene, phyllosilicate, carbonate, and organic concentrations between grains of SM2 and SM12 and across single grains at micron scale. Raman spectra indicate higher-temperature metamorphism for SM12 than SM2, suggesting inhomogeneous temperate distribution across the SM parent body.

Acknowledgments: Thanks to P. Jenniskens and D. Sears for the Sutter's Mill samples. SRC is funded by the University of Wisconsin-Madison, user's fees, and the University of Wisconsin-Milwaukee. The IRENI beamline was developed under NSF 0619759. M. Yesiltas is supported by Turkish Graduate Fellowship #1416.

References: [1] Jenniskens, P. et al. (2012) *Science* 338, 1583; [2] Nasse, M. J., et al. (2011) *Nature Methods* 8, 413; [3] Cody G. D. et al. (2008) *Earth and Planet. Sci. Letters* 272, 446; [4] Sandford, S. A. et al. (2013) *LPS XXXXIV*, 1163; [5] Yesiltas, M. et al. (2013) *76th Ann. Met. Soc. Mtg.*, Abstract #5068; [6] Yesiltas, M. et al. (2013) *LPS XXXXIV*, Abstract #2717.